11th International Symposium on Magnetic Bearings
August 26-29, Nara, Japan

TRANSIENT DROP ANALYSIS OF AUXILIARY BEARINGS IN FLUID FILM/MAGNETIC BEARING SUPPORTED ROTOR

Amir A. Younan, Tim W. Dimond and Paul E. Allaire
Mechanical and Aerospace Engineering Department, University of Virginia, Charlottesville VA 22904, USA
aay7n@virginia.edu, twd5c@virginia.edu and pea@virginia.edu

ABSTRACT

The work focuses on the design of the auxiliary bearings for the primary magnetic system in a new fluid film bearing test rig. The design is unique since the rotor is supported by the central tested journal bearing along with the two magnetic bearings. A three mass model for the rig is used to conduct the transient analysis of the rotor drop. Hertz contact theory is used to describe the contact between the rotor and the inner race of the back-up bearings. The analysis included different sets of auxiliary bearings as well as different levels of damping.

INTRODUCTION

An AMB auxiliary bearing system is designed to support the rotor in the case of support loss of AMB. The auxiliary bearing is placed in the stator part of the system and it is not active during normal operation. The inactivity of the auxiliary bearing is achieved by the existence of a clearance between the inner race of the bearing and the rotor surface. Typically, fifty percent of the magnetic bearing air gap [1] is used for the back-up bearing clearance. The drop analysis is governed by the forces on the rotor (weight and unbalance forces), auxiliary bearing properties (stiffness and damping coefficients) and the rotor/stator contact properties (friction, contact stiffness and damping coefficients). The desirable behavior is that the rotor simply drops then oscillates back and forth a few times in the auxiliary bearing without large amplitude whirling. This behavior should result in little or no damage in the machine [2].

Ishii and Kirk [1] formulated a simplified rotordynamic model for an AMB compressor. The model consisted of several masses and took into consideration the flexibility of the bearing and the housing. The contact model was evaluated using Hertzian contact theory. A transient analysis was conducted in order to track the behavior of the shaft before, during and after the drop. Zeng et al [3] extended the work of Ishii and Kirk to include the effects of the rubbing between the rotor and the compressor seal on the drop analysis.

This work studies the rotor drop analysis of a new fluid film bearing test rig, Figure 1. The primary support system of the test rig consists of two magnetic bearings, which are also used as actuators to test the journal bearing dynamic coefficients. The tested journal bearing is mounted in the center of the shaft between the two magnetic bearings. The auxiliary bearings are installed at both ends of the shaft to catch the rotor in the case of AMB power loss. The target of this drop analysis was to design the appropriate bearings for the new test rig. The rotor drop analysis will generally follow the work presented in [1] and [3]. The auxiliary bearing design will be unique since the tested journal bearing will provide a central support for the shaft during drop. The existing stiffness and damping coefficients of the bearing will help in reducing the impact of the rotor on the auxiliary bearing. Several stiffness and damping values are studied in the analysis to be able to select the best auxiliary bearing design appropriate for the fluid film test rig.

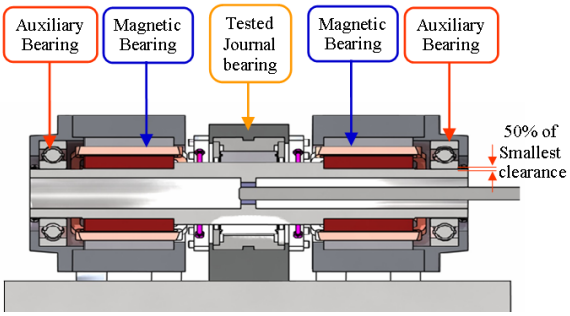

FIGURE 1: Sectional view of the testing section

ROTOR MODEL OF THE TEST RIG

The test rig consists of a rigid rotor with a diameter of 0.127 m (5 in.) and length of 0.743 m (29.25 in.). The rotor is modeled as three mass rotor as seen in Figure 2. The rotor mass is modeled mainly as a central mass

(M_2) since the rotor runs below the first critical bending speed. The magnetic bearing laminations and the shaft mass inside each of the auxiliary bearing are modeled as two masses (M_1 and M_3) at each end of the shaft

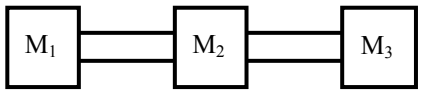

FIGURE2: Layout of the three mass model of the rotor

The motion of each mass is described by three degrees of freedom: Two lateral displacements (X, Y) and one angular displacement (θ) about the axis of the rotor. The lateral displacements capture the whirling motion of the masses inside the auxiliary bearing clearance.
The rotational degree of freedom describes the effects of the impact and friction on the shaft rotational speed during rotor drop.
The rotor analysis has two cases: before the rotor drop and after the rotor drop. Before the rotor drop, the shaft is supported by the two magnetic bearing and the journal bearing, as shown in Figure 3. After the drop, the rotor starts to interact with the auxiliary bearing while still being supported by the journal bearing. The interaction of the shaft with the inner race of the auxiliary bearing is described by the normal and tangential contact forces. The contact forces are function of the stiffness and damping properties of the Hertzian contact area.

GOVERNING EQUATIONS

Central mass before the rotor drop

The central mass M_2 is supported by the damping (C_{xx}) and (C_{yy}) and stiffness (K_{xx}) and (K_{yy}) coefficients of the journal bearing as illustrated in Figure 4. The shaft lateral (K_s) and torsional stiffness ($K_{s\theta}$) relative to the end masses also contribute in the motion of the central mass. Finally, the lateral and torsional structural damping are modeled as two dampers (C_s) and ($C_{s\theta}$) respectively.
The shaft stiffness is calculated from the deflection of a shaft holding three masses as developed in [4].

$$K_s = \frac{12EI}{L^3}\begin{bmatrix} 1 & -2 & 1 \\ -2 & 4 & -2 \\ 1 & -2 & 1 \end{bmatrix} \qquad (1)$$

The center of gravity of the central mass (M_2) was assumed to be located at a distant e_u from the geometric center. The eccentricity (e_u) results from the unbalance forces in the rotor.

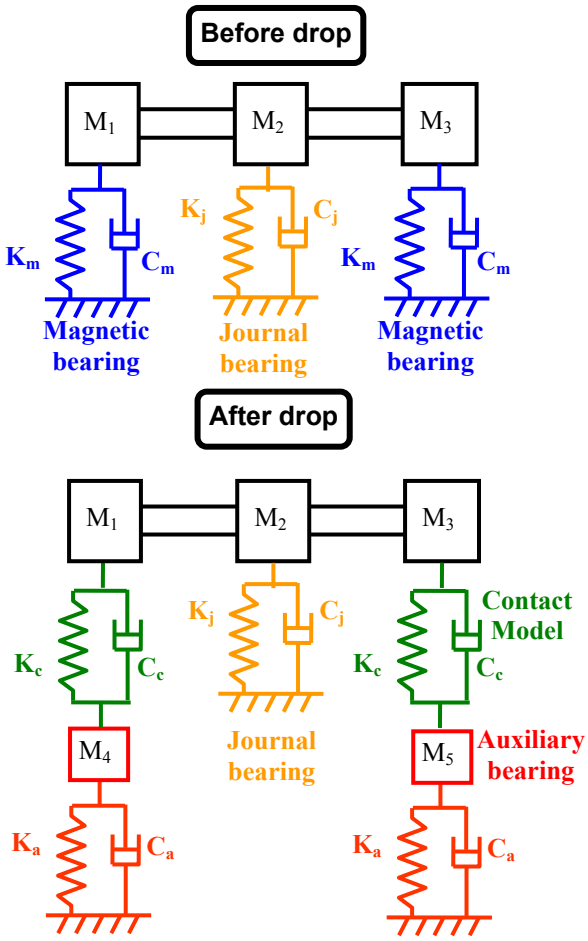

FIGURE 3: Schematic of the rotor before/after the drop

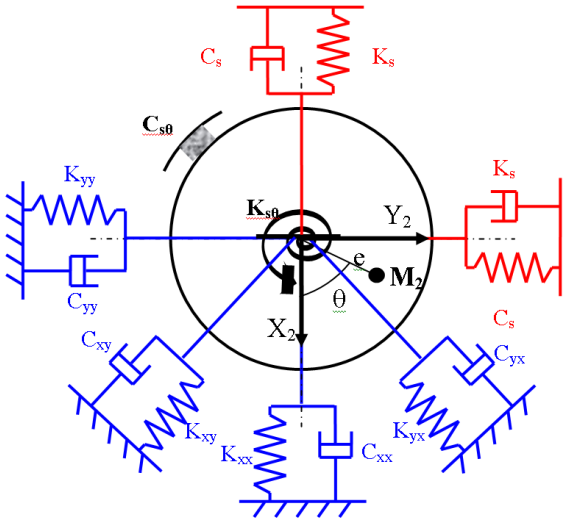

FIGURE 4: Representation of the forces acting on the central mass M_2

The relation between the coordinates of the center of gravity ($X_{c.g.}$, $Y_{c.g.}$) and the geometric center can be formulated as follows:

$$X_{c.g.2} = X_2 + e_u \cos(\theta_2)$$
$$Y_{c.g.2} = Y_2 + e_u \sin(\theta_2) \qquad (2)$$

The velocity and the acceleration of the center of gravity

$$\dot{X}_{c.g.2} = \dot{X}_2 - e_u \dot{\theta}_2 \sin\theta_2$$
$$\ddot{X}_{c.g.2} = \ddot{X}_2 - e_u \ddot{\theta}_2 \sin\theta_2 - e_u \dot{\theta}_2^{\,2} \cos\theta_2$$
$$\dot{Y}_{c.g.2} = \dot{Y}_2 + e_u \dot{\theta}_2 \cos\theta_2 \qquad (3)$$
$$\ddot{Y}_{c.g.2} = \ddot{Y}_2 + e_u \ddot{\theta}_2 \cos\theta_2 - e_u \dot{\theta}_2^{\,2} \sin\theta_2$$

The equation of motion of the central mass is best formulated using Lagrange formulation in order to be able to capture the eccentricity of the center of gravity. The equations in x, y and θ can be written as follows:

$$M_2\left(\ddot{X}_2 - e_u\ddot{\theta}_2\sin\theta_2 - e_u\dot{\theta}_2^{\,2}\cos\theta_2\right) + C_{xx}\dot{X}_2 + C_{xy}\dot{Y}_2$$
$$+C_s(4\dot{X}_2 - 2\dot{X}_1 - 2\dot{X}_3) + K_{xx}X_2 + K_{xy}Y_2$$
$$+K_s(4X_2 - 2X_1 - 2X_3) - M_2 g = 0$$

$$M_2\left(\ddot{Y}_2 + e_u\ddot{\theta}_2\cos\theta_2 - e_u\dot{\theta}_2^{\,2}\sin\theta_2\right) + C_{yy}\dot{Y}_2 + C_{yx}\dot{X}_2$$
$$+C_s(4\dot{Y}_2 - 2\dot{Y}_1 - 2\dot{Y}_3) + K_{yy}Y_2 + K_{yx}X_2$$
$$+K_s(4Y_2 - 2Y_1 - 2Y_3) = 0$$

$$\left(M_2 e_u^{\,2} + J_2\right)\ddot{\theta}_2 + C_{s\theta}(2\dot{\theta}_2 - \dot{\theta}_1 - \dot{\theta}_3) + K_{s\theta}(2\theta_2 - \theta_1 - \theta_3)$$
$$+M_2\left(\left(-\ddot{X}_2 - \dot{Y}_2\dot{\theta}_2\right)e_u\sin\theta_2 + \left(\ddot{Y}_2 - \dot{X}_2\dot{\theta}_2\right)e_u\cos\theta_2\right)$$
$$+M_2 g e_u \sin\theta_2 = 0 \qquad (4)$$

Two end masses before the rotor drop

The motion of these masses (M_1 and M_3) is governed by the magnetic bearing stiffness (K_m) and damping (C_m) forces. The response is also affected by the motion of the central mass M_2 through the stiffness and damping of the shaft. The equations for mass M_1 and M_3 in x, y and θ can be written as follows:

$$M_1\ddot{X}_1 + C_s(\dot{X}_1 - 2\dot{X}_2 + \dot{X}_3) + C_m\dot{X}_1 + K_s(X_1 - 2X_2 + X_3)$$
$$+K_m X_1 - M_1 g = 0$$
$$M_1\ddot{Y}_1 + C_s(\dot{Y}_1 - 2\dot{Y}_2 + \dot{Y}_3) + C_m\dot{Y}_1 + K_s(Y_1 - 2Y_2 + Y_3)$$
$$+K_m Y_1 = 0$$
$$J_1\ddot{\theta}_1 + C_{s\theta}(\dot{\theta}_1 - \dot{\theta}_2) + K_{s\theta}(\theta_1 - \theta_2) = 0 \qquad (5)$$

$$M_3\ddot{X}_3 + C_s(\dot{X}_3 - 2\dot{X}_2 + \dot{X}_1) + C_m\dot{X}_3 + K_s(X_3 - 2X_2 + X_1)$$
$$+K_m X_3 - M_3 g = 0$$
$$M_3\ddot{Y}_3 + C_s(\dot{Y}_3 - 2\dot{Y}_2 + \dot{Y}_1) + C_m\dot{Y}_3 + K_s(Y_3 - 2Y_2 + Y_1)$$
$$+K_m Y_3 = 0$$
$$J_3\ddot{\theta}_3 + C_{s\theta}(\dot{\theta}_3 - \dot{\theta}_2) + K_{s\theta}(\theta_3 - \theta_2) = 0 \qquad (6)$$

Contact force and deflection equation

When the magnetic bearing is inactive, the rotor drop analysis starts to account for the impact of the shaft inside the available clearance of the auxiliary bearing. Figure 5 shows the contact forces which arise at the auxiliary bearing impact points. The contact forces are the normal contact force (F_n) and the tangential contact force (F_t). They depend on the Hertzian contact stiffness (K_c) and damping (C_c) coefficients as well as the amount of elastic deflection (δ) of the inner race of the bearings.

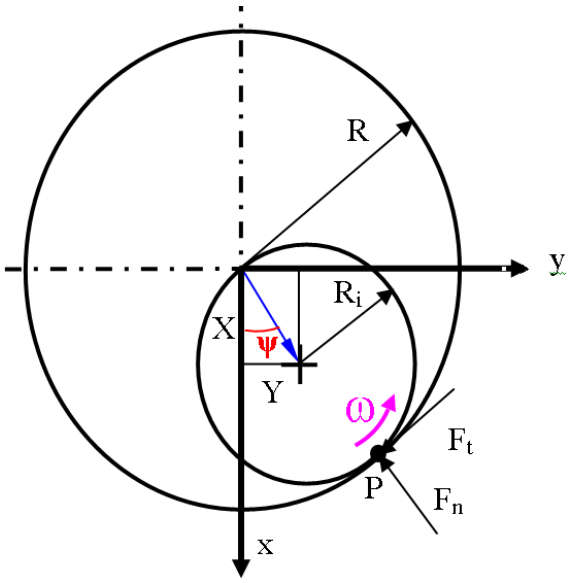

FIGURE 5: Representation of the end mass inside the back-up bearing

$$F_n = K_c\delta + C_c\dot{\delta}, F_t = \mu F_n \qquad (8)$$

The deflection is calculated by subtracting the radial motion from the clearance. The angular position of the penetration is ψ

$$\delta = \sqrt{X^2 + Y^2} - (R_o - R_i) \quad \dot{\delta} = \frac{X\dot{X} + Y\dot{Y}}{\sqrt{X^2 + Y^2}}$$
$$\psi = \tan^{-1}\frac{Y}{X} \qquad (9)$$

Central mass after the rotor drop

The equation of motion for the central mass will involve the contact forces between the shaft and the inner surface of the journal bearing. It is important to mention that the clearance of the auxiliary bearing is less than the clearance of the journal bearing. The main reason is to try to protect the babbitt surface on the inner surface of the journal. If the journal bearing remains in action the contact force N_2 will be zero. The equation will be formed from equation (4). The normal force for the central mass is N_2 and its angular position is ψ_2 as derived in equation (8) and (9). The radius of the shaft inside the journal bearing is R_2.

$$
\begin{aligned}
&M_2\left(\ddot{X}_2 - e\ddot{\theta}_2 \sin\theta_2 - e\dot{\theta}_2^2 \cos\theta_2\right) + C_{xx}\dot{X}_2 + C_{xy}\dot{Y}_2 \\
&+C_s(4\dot{X}_2 - 2\dot{X}_1 - 2\dot{X}_3) + K_{xx}X_2 + K_{xy}Y_2 \\
&+K_s(4X_2 - 2X_1 - 2X_3) = -N_2(\cos(\psi_2) - \mu_2\sin(\psi_2)) + M_2 g \\
&M_2\left(\ddot{Y}_2 + e\ddot{\theta}_2 \cos\theta_2 - e\dot{\theta}_2^2 \sin\theta_2\right) + C_{yy}\dot{Y}_2 + C_{yx}\dot{X}_2 + \\
&C_s(4\dot{Y}_2 - 2\dot{Y}_1 - 2\dot{Y}_3) + K_{yy}Y_2 + K_{yx}X_2 \\
&+K_s(4Y_2 - 2Y_1 - 2Y_3) = -N_2(\sin(\psi_2) + \mu_2\cos(\psi_2))
\end{aligned}
$$

$$
\begin{aligned}
&\left(M_2 e^2 + J_2\right)\ddot{\theta}_2 + C_{s\theta}(2\dot{\theta}_2 - \dot{\theta}_1 - \dot{\theta}_3) + K_{s\theta}(2\theta_2 - \theta_1 - \theta_3) \\
&+M_2\left(\left(-\ddot{X}_2 - \dot{Y}_2\dot{\theta}_2\right)e\sin\theta_2 + \left(\ddot{Y}_2 - \dot{X}_2\dot{\theta}_2\right)e\cos\theta_2\right) \\
&+M_2 ge\sin\theta_2 = -\mu_2 N_2 R_2 \qquad (10)
\end{aligned}
$$

Two end masses after the rotor drop

After the drop, the two end masses start to bump inside the inner race of the auxiliary bearing. The same form of the contact forces are added to the two end masses equations (8) and (9).

$$
\begin{aligned}
&M_1\ddot{X}_1 + C_s(\dot{X}_1 - 2\dot{X}_2 + \dot{X}_3) + K_s(X_1 - 2X_2 + X_3) \\
&+C_m\dot{X}_1 + K_m X_1 = -N_1(\cos(\psi_1) - \mu_1\sin(\psi_1)) + M_1 g \\
&M_1\ddot{Y}_1 + C_s(\dot{Y}_1 - 2\dot{Y}_2 + \dot{Y}_3) + K_s(Y_1 - 2Y_2 + Y_3) \\
&+C_m\dot{Y}_1 + K_m Y_1 = -N_1(\sin(\psi_1) + \mu_1\cos(\psi_1)) \\
&J_1\ddot{\theta}_1 + C_{s\theta}(\dot{\theta}_1 - \dot{\theta}_2) + K_{s\theta}(\theta_1 - \theta_2) = -N_1\mu_1 R_1
\end{aligned}
\qquad (11)
$$

$$
\begin{aligned}
&M_3\ddot{X}_3 + C_s(\dot{X}_3 - 2\dot{X}_2 + \dot{X}_1) + K_s(X_3 - 2X_2 + X_1) \\
&+C_m\dot{X}_3 + K_m X_3 = -N_3(\cos(\psi_3) - \mu_3\sin(\psi_3)) \\
&M_3\ddot{Y}_3 + C_s(\dot{Y}_3 - 2\dot{Y}_2 + \dot{Y}_1) + K_s(Y_3 - 2Y_2 + Y_1)_3 \\
&+C_m\dot{Y}_3 + K_m Y = -N_3(\sin(\psi_3) + \mu_3\cos(\psi_3)) \\
&J_3\ddot{\theta}_3 + C_{s\theta}(\dot{\theta}_3 - \dot{\theta}_2) + K_{s\theta}(\theta_3 - \theta_2) = -N_3\mu_3 R_3
\end{aligned}
\qquad (12)
$$

Two auxiliary bearing masses after the rotor drop

The motion of the auxiliary bearing masses (M_4 and M_5) is governed by the stiffness and damping forces of the auxiliary bearing as well as the contact forces generated from the impact of the shaft with the inner race of the bearing. The auxiliary bearing mass (M_4) under the end mass (M_1)

$$
\begin{aligned}
&M_4\ddot{X}_4 + C_b(\dot{X}_4 - \dot{X}_1) + K_b(X_4 - X_1) \\
&= N_1(\cos(\psi_1) - \mu_1\sin(\psi_1)) \\
&M_4\ddot{Y}_4 + C_b(\dot{Y}_4 - \dot{Y}_1) + K_b(Y_4 - Y_1) \qquad (13) \\
&= N_1(\sin(\psi_1) + \mu_1\cos(\psi_1)) \\
&J_4\ddot{\theta}_4 + C_{b\theta}\dot{\theta}_4 = \mu_1 N_1 R_1
\end{aligned}
$$

The auxiliary bearing mass (M_5) under the end mass (M_3)

$$
\begin{aligned}
&M_5\ddot{X}_5 + C_b(\dot{X}_5 - \dot{X}_3) + K_b(X_5 - X_3) \\
&= N_3(\cos(\psi_3) - \mu_3\sin(\psi_3)) \\
&M_5\ddot{Y}_5 + C_b(\dot{Y}_5 - \dot{Y}_3) + K_b(Y_5 - Y_3) \\
&= N_3(\sin(\psi_1) + \mu_3\cos(\psi_3)) \qquad (14) \\
&J_5\ddot{\theta}_5 + C_{b\theta}\dot{\theta}_5 = \mu_3 N_3 R_3
\end{aligned}
$$

Normal force calculation for each mass

The normal force was derived in equation (8) as a function of the elastic deflection (9). The calculation of the contact force for the central mass is as follows

$$
N_2 = K_c\delta_2 + C_c\dot{\delta}_2 \qquad F_{t2} = \mu_2 N_2 \qquad (15)
$$

$$
\delta_2 = \sqrt{X_2^2 + Y_2^2} - (R_{2c} - R_2) \qquad \dot{\delta} = \frac{X_2\dot{X}_2 + Y_2\dot{Y}_2}{\sqrt{X_2^2 + Y_2^2}}
$$

$$
\psi_2 = \tan^{-1}\frac{Y_2}{X_2} \qquad (16)
$$

The R_{2c} is the journal bearing radius at the central mass location. It is equal to the rotor diameter R_2 added to the radial clearance of the journal bearing. The normal force of the two auxiliary bearings depends on the motion of the end masses as well as the motion of the bearing as follows:

$$
N_1 = K_c\delta_1 + C_c\dot{\delta}_1 \qquad F_{t1} = \mu_1 N_1 \qquad (17)
$$

$$
\delta_1 = \sqrt{\left(X_1 - X_4\right)^2 + \left(Y_1 - Y_4\right)^2} - (R_{1b} - R_1)
$$

$$
\dot{\delta}_1 = \frac{\left(X_1 - X_4\right)\dot{X}_1 + \left(X_4 - X_1\right)\dot{X}_4 + \left(Y_1 - Y_4\right)\dot{Y}_1 + \left(Y_4 - Y_1\right)\dot{Y}_4}{\sqrt{\left(X_1 - X_4\right)^2 + \left(Y_1 - Y_4\right)^2}}
$$

$$
\psi_1 = \tan^{-1}\frac{Y_1 - Y_4}{X_1 - X_4} \qquad (18)
$$

$$N_3 = K_c\delta_3 + C_c\dot{\delta}_3 \qquad F_{t3} = \mu_3 N_3 \qquad (19)$$

$$\delta_3 = \sqrt{(X_3 - X_5)^2 + (Y_3 - Y_5)^2} - (R_{3b} - R_3)$$

$$\dot{\delta}_3 = \frac{(X_3 - X_5)\dot{X}_1 + (X_5 - X_3)\dot{X}_5 + (Y_3 - Y_5)\dot{Y}_3 + (Y_5 - Y_3)\dot{Y}_5}{\sqrt{(X_3 - X_5)^2 + (Y_3 - Y_5)^2}}$$

$$\psi_3 = \tan^{-1}\frac{Y_3 - Y_5}{X_3 - X_5} \qquad (20)$$

Here R_{1c} and R_{3c} are the radii of the inner race of the auxiliary bearing. They are equal to the radial clearance of the auxiliary bearing added to the rotor diameter R_1 and R_3 respectively.

Coefficient of friction

The tangential contact force has always the opposite direction of the moving surface velocity. The direction of the force will be determined from the relative velocity of the two contact surfaces. Inside the auxiliary bearing, the two relative velocities are the angular velocity of the shaft and the angular velocity of the inner race of the auxiliary bearing. The static sliding coefficient of friction is μ_s and the sliding coefficient of friction is μ_d.

$$V_{1shaft} = R_1\dot{\theta}_1 - \dot{X}_1\sin(\psi_1) + \dot{Y}_1\cos(\psi_1)$$

$$V_{4brg} = R_{1c}\dot{\theta}_4 - \dot{X}_4\sin(\psi_1) + \dot{Y}_4\cos(\psi_1)$$

$$\mu_1 = \begin{cases} \mu_d & V_{1shaft} > V_{4brg} \\ \mu_s & V_{1shaft} = V_{4brg} \\ -\mu_d & V_{1shaft} < V_{4brg} \end{cases} \qquad (21)$$

$$V_{3shaft} = R_3\dot{\theta}_3 - \dot{X}_3\sin(\psi_3) + \dot{Y}_3\cos(\psi_3)$$

$$V_{5brg} = R_{3c}\dot{\theta}_5 - \dot{X}_5\sin(\psi_3) + \dot{Y}_5\cos(\psi_3)$$

$$\mu_3 = \begin{cases} \mu_d & V_{3shaft} > V_{5brg} \\ \mu_s & V_{3shaft} = V_{5brg} \\ -\mu_d & V_{3shaft} < V_{5brg} \end{cases} \qquad (22)$$

ANALYSIS STEPS

The analysis strategy is to predict the motion and the behavior of the motor following the loss of the magnetic support system. The analysis is devised into two subsequent steps as shown in figure 6. The first is to study the steady state response of the system under normal operating condition: the magnetic support is active and the unbalance force is applied. The second part starts with the loss of the magnetic bearing and the start of the transient analysis of the rotor drop. The analysis assumes that the magnetic bearing is not effective after the drop. The first part of the analysis is governed by equations (4), (5) and (6) which describe the three degrees of freedom of each of the three rotor masses (9 degrees of freedom). The system of equation can be described in a state space representation using the position and velocity of each degree of freedom. The total number of state variables S is 18. The initial conditions for the states are zero.

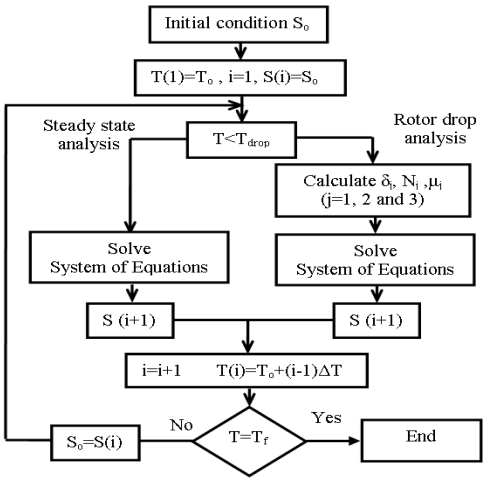

FIGURE 6: Flow chart of the transient analysis of the rotor drop

The second part involves the two auxiliary bearing masses as well as the three rotor masses. At each step, the deflection for each mass is calculated and the normal forces and their direction are determined as in equations (16-20). The transient response after the drop is governed by 15 equations for the three degrees of freedom of the five masses. The system of equation can be also described in a state space representation using the position and velocity of each degree of freedom. The total number of state variables is 30.

TRANSIENT ANALYSIS

The rotor drop analysis is conducted on the fluid film test rig rotor configuration. The rotor data is summarized in Table 1. The transient analysis is conducted over a period of 0.3 second. The initial time is zero and the rotor drop takes place at 0.1 sec. The time of the drop was selected so that the rotor reached its steady state position while subject to the unbalance force. The time step was $1x10^{-5}$ second.

The analysis is conducted for two cases: The first case assumes that the journal bearing remains active after the drop and hence helped support the rotor during the drop. The second is a worse case scenario where the drop

occurs without any support from the journal bearing. The second case is studied in the case where the journal bearing coefficients are greatly reduced due to the large movement of the shaft.

Table 1: Fluid film test rig data

Central Mass M_2	14.9 Kg
End Mass Weight $M_{1\&3}$	14.9 Kg
Mass moment of Inertia J_2	0.149 kg.m^2
Mass moment of Inertia $J_{1\&3}$	0.083 Kg.m^2
Eccentricity e_u	5.73x10^{-7} m
Aux. bearing Mass $M_{4\&5}$	2 Kg
Aux. bearing moment of Inertia $J_{4\&5}$	0.01 Kg.m^2
Bearing stiffness K_{xx}	2.17x10^9 N/m
Bearing stiffness K_{xy}	2.31x10^6 N/m
Bearing stiffness K_{yx}	13.86x10^6 N/m
Bearing stiffness K_{yy}	2.17x10^9 N/m
Bearing Damping C_{xx}	803x10^3 N.s/m
Bearing Damping C_{xy}	2276 N.s/m
Bearing Damping C_{yx}	-210 N.s/m
Bearing Damping C_{yy}	803x10^3 N.s/m
Shaft Stiffness Ks	114x10^6 N/m
Shaft torsional stiffness Ksθ	1x10^6 N.m/rad
Shaft structural damping Cs	1646.9 N.s/m
Shaft torsional damping $C_{s\theta}$	15.56 N.s/m
Aux. bearing stiffness K_b	1x10^7-5x10^7 N/m
Aux. bearing damping C_b	200-2000 N.s/m
Aux. bearing torsional damping $C_{b\theta}$	1x10^{-4} N.s/m
Contact stiffness K_c	5x10^8 N/m
Contact damping C_c	200 N/m
Magnetic bearing stiffness K_m	1.75x10^7 N/m
Magnetic bearing damping C_m	1000 N.s/m
Running speed	22000 rpm
Friction coefficient	0.2
Static Friction coefficient	0.5
Aux. bearing coefficient of friction	0.0015

First case with journal bearing

Figure 7 illustrates the behavior of the rotor during the drop while the journal bearing is active: The first row represents the response of mass M_1, the second row represents the response of mass M_2 and the third row represents the response of mass M_3. The columns represent the progress in time. The first column is the response before the drop (0 sec to 0.1 sec).

The second column represents the response after the drop from 0.1 to 0.3 sec. The lines in purple represent the response of the previous step in time. In the first column of plots in Figure 7, the masses start from rest and reach the steady state response of the system due to the unbalance force on the central mass M_2. The response is oscillatory due to the harmonic behavior of the force.

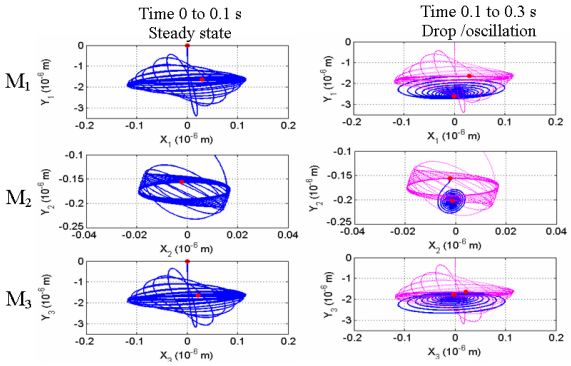

FIGURE 7: Transient response of the rotor using the first set of journal bearing coefficient

In the second column of plots, the rotor is dropped and the magnetic support properties are set to zero. The rotor is now solely supported by the central journal bearing. The response of the rotor is damped due to the large damping coefficient of the journal bearing {O (1x10^{5}N.s/m)} and the stiffness coefficient {O (1x10^{9}N/m)}. The effective damping ratio is less than one and the system behaves as an underdamped free vibration system.

Second case without journal bearing

In this case, the rotor losses its magnetic supports as well as the journal bearing support. Two level of stiffness were tested for auxiliary bearing at two damping levels. The first is a less stiff auxiliary bearing set with stiffness K_b (1x10^7 N/m) and the second represents a stiffer bearing set with stiffness K_b (5x10^7 N/m). The two levels of bearing damping are 200 and1000 N.s/m respectively.

Auxiliary bearing stiffness (K_b=1x10^7 N/m). The first column in Figure 8 illustrates the steady state response of the rotor for the unbalance force. In the first time interval, the journal bearing and the magnetic bearings support the rotor. At the end of the first interval, the rotor is dropped (at 0.1 sec). Both supports are lost (their stiffness and damping coefficients are set to zero) and the rotor is only supported by the auxiliary bearing through the impact with its inner race.

In the second column, the circle represents the clearance space between the rotor and the inner race of the auxiliary bearing for M_1 and M_3. For the central mass M_2, the circle represents the clearance between the rotor

and the pads of the journal bearing. The initial conditions for the drop are the steady state response in the first column. The rotor is dropped as seen vertically downward to hit the inner races.

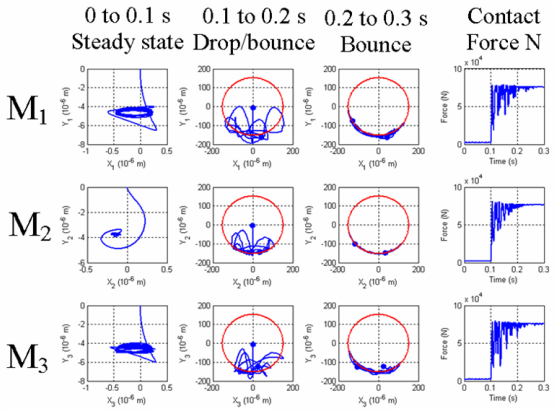

FIGURE 8: Transient response of the rotor for auxiliary bearing stiffness 10^7 N/m and damping 200 N.s/m

The rotor starts to bounce in the bottom half of the auxiliary bearing. Due to the low damping in this case, we can see that the bouncing distance is relatively large. However, after 0.2 sec, the rotor starts to rest relatively quietly on the bottom of inner race. The fourth column shows the contact force. During the first 0.1 sec, there is no contact between the rotor and inner race. At the rotor drop, the force starts with an impulse of the impact of the rotor in the inner race. The contact force is approximately 80 kN for each impact. This magnitude depends on the weight of the rotor as well as the dynamic forces. During the rotor bounce, the normal contact force starts dropping to zero until the next impact which takes it back near the 80 kN level.

Figure 9 illustrates the rotor response with a higher level of damping in the auxiliary bearing (1000 N.s/m). Since the steady state response is the same as the previous case, the initial conditions for the drop is exactly the same.

In the second column, the bouncing response is less than Figure 8 due to the presence of the higher damping level. The rotor center motion crosses the circle. The crossing represents the amount of deflection of the inner race. Due to the presence of the damping, the rotor remains in contact with the auxiliary bearing for a longer period of time. From 0.2 -0.3 sec, the rotor starts to move as one body in a backward whirl motion. The backward whirl can be seen in the motion of the three masses. The contact force remains almost constant at 80 kN during the backward whirl. The inner race deflection and the backward whirl are two signs of probable damage that will take place in the real test rig at this stiffness level.

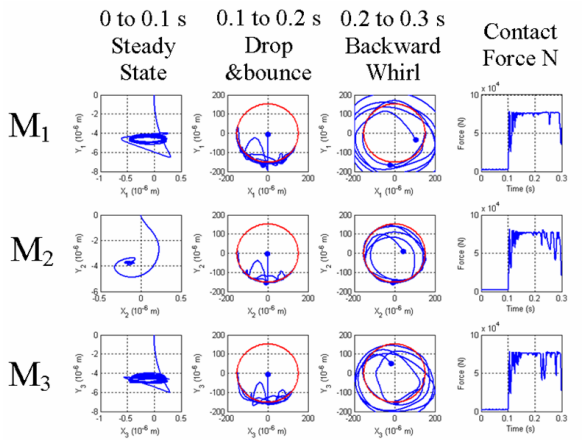

FIGURE 9: Transient response of the rotor for auxiliary bearing stiffness 1x10^7 N/m and damping 1000 N.s/m

Auxiliary bearing stiffness (K_b=5x10^7 N/m). Figure 10 and 11 describe the transient response of the rotor with a stiffener bearing for two damping levels. The rows correspond to the response of M_1, M_2 and M_3 respectively. The steady state response in the first column is again exactly the same responses in the case of K_b 1x10^7 N/m. The bounce of the rotor from the impact is higher than the softer case. The frequency of the impact is higher due to the higher stiffness of the auxiliary bearing. Due to the small amount of damping, the impact response is rapid and the rotor doesn't remain in touch with the inner race.

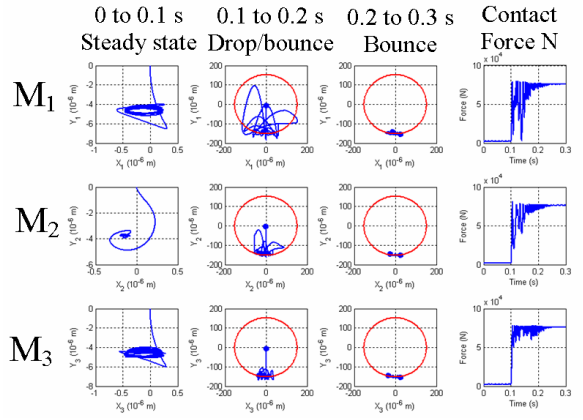

FIGURE 10: Transient response of the rotor for auxiliary bearing stiffness 5x10^7 N/m and damping 200 N.s/m

It is important to mention that the motion of the masses M_1 and M_3 are different due to the randomness of the motion of the drop after the impact. This difference is the reason for taking the motion of the two masses into account. The motion in this case has a conical shape where M_1 is bouncing inside the clearance while M_3 represents a pivot on the other end of the rotor. For these two cases, the motion was damped out in 0.2 seconds. The backward whirl was not depicted in the stiff auxiliary bearing (K_b= 5x10^7 N/m) for the two damping levels.

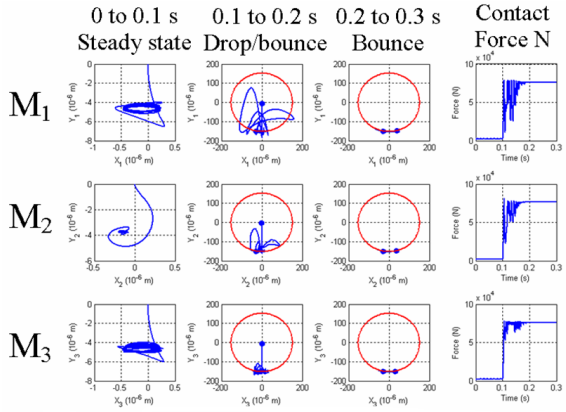

FIGURE 11: Transient response of the rotor for auxiliary bearing stiffness 5x10^7 N/m and damping 1000 N.s/m

CONCLUSIONS

The rotor drop analysis is presented for the fluid film test rig for an AMB failure. The three-mass model was able to capture the transient motion of the two ends masses. From Figures (10)-(11), the motion of these two masses were found to be different due to the randomness of the response after the first impact. The Hertzian contact model was implemented at the impact point. The normal and tangential contact forces were functions of the Hertzian contact stiffness, contact damping and the coefficient of friction.

The journal bearing was able to provide a central support to the rotor and prevent impact. The behavior of the rotor depends on the damping as well as the stiffness of the journal bearing.

An additional analysis was conducted in the case where the journal bearing fails to support the shaft. The low stiffness auxiliary bearing allows a higher response at the auxiliary bearing at the rotor drop than the stiff auxiliary bearings. A backward whirl was identified in the presence of high damping (1000 N.s/m). As a solution for the identified backward whirl, the case of a higher stiffness auxiliary bearing was analyzed. The rotor in this case bounces on the bottom half of the inner race. The response is damped out in 0.2 sec. The analysis without the journal bearing was able to predict the magnitude of the contact forces during the rotor drop. The magnitude of the normal contact forces remains in the same range of 80 kN. The suitable auxiliary bearing design is a pair of rolling element bearing at each side of the rotor. The pair will provide a high stiffness for the support which will prevent the backward whirl and reduce the amount of bouncing during the rotor drop.

REFERENCES

1. Ishii T, Kirk R G., (1996), “Transient response technique applied to active magnetic bearing machinery during rotor drop”. Journal of Vibration &Acoustics, 118(2), pp. 154–163.

2. Foils, W. C. and Allaire, P. E., (1997), “Nonlinear transient modeling of active magnetic bearing rotor during rotor drop on auxiliary bearing”. Proceedings of MAG’97, Alexandria, USA, pp 154–163.

3. Ji, Jinchen and Yu, Lie (2000) “Drop Dynamics of a High-Speed Unbalanced Rotor in Active Magnetic Bearing Machinery”, Mechanics Based Design of Structures and Machines, 28(2), pp185 – 200.

4. Allaire, P., Pilkey W., (2004) “Mechanical Vibration Course Notes”, University of Virginia, Section 5.